

INTERACTION OF LASER RADIATION WITH MATTER

PACS numbers: 42.62.Cf; 73.20.Mf
DOI: 10.1070/QE2014v044n04ABEH015219

Formation of micron and submicron structures on a zirconium oxide surface exposed to nanosecond laser radiation

D.V. Ganin, S.I. Mikolutskiy, V.N. Tokarev, V.Yu. Khomich, V.A. Shmakov, V.A. Yamshchikov

Abstract. **Possibility of forming quasi-periodic structures of micron and submicron dimensions on a surface of zirconium dioxide under the action of eximer ArF laser radiation is shown experimentally and theoretically.**

Keywords: *nanosecond laser radiation, zirconium dioxide, submicron structures, thermal stress.*

1. Introduction

Development of hydrogen energetics as an ecologically pure and highly efficient source of thermal and electrical energy attracts active interest nowadays. A most important problem in this field is obtaining electrical energy by means of solid oxide fuel cells (SOFCs). Solving this problem may substantially increase the efficiency of thermal power stations.

Zirconium dioxide possessing a cubic crystal structure stabilised by yttrium oxide impurities is employed as a material for producing electrolytic membranes in SOFCs due to its high chemical stability, strength, and conductivity for oxygen ions at high temperatures.

For enhancing the efficiency of SOFCs it is necessary to increase a flux of oxygen ions through their membrane. This may be achieved by forming micron and submicron roughness on the membrane surface. This process may be simplified by employing so-called direct laser nanostructuring which helps surface processing in a simplest way by using a single laser beam without any auxiliary and expensive arrangements and devices [1–7]. Note that employment of nanosecond lasers for this purpose has advantages of low price and simple service as compared to pico- and femtosecond radiation sources.

For controlling the period and dimensions of surface structures produced in this way it is necessary to understand the nature of occurring processes. This is why experiments in the present work are accompanied by a theoretical model of formation of structures with micron and submicron dimensions on the material under study due to nonlinear relaxation of laser-induced thermal stresses.

D.V. Ganin Physics Instrumentation Center, A.M. Prokhorov General Physics Institute, Russian Academy of Sciences, 142190 Troitsk, Moscow, Russia; e-mail: ganin@pic.troitsk.ru;
S.I. Mikolutskiy, V.Yu. Khomich, V.A. Yamshchikov Institute for Electrophysics and Electric Power, Russian Academy of Sciences, Dvortsovaya nab. 18, 191186 St. Petersburg, Russia
e-mail: mikolserg@mail.ru, Khomich@ras.ru, yamschikov52@mail.ru;
V.N. Tokarev, V.A. Shmakov A.M. Prokhorov General Physics Institute, Russian Academy of Sciences, ul. Vavilova 38, 119991 Moscow, Russia; e-mail: vtokarev56@mail.ru, shmakovv@mtu-net.ru

Received 27 April 2013; revision received 7 November 2013
Kvantovaya Elektronika **44** (4) 317–321 (2014)
Translated by N.A. Raspopov

2. Experimental

In direct laser nanostructuring we employed a nanosecond ArF laser with a radiation wavelength of 193 nm, pulse duration of 25 ns, pulse energy of 200 mJ, and pulse repetition rate of up to 100 Hz. As an irradiated material we used plates made of 'fianite'. Physicochemically, this material is zirconium dioxide with a cubic crystal structure stabilised by an yttrium oxide impurity. The content of yttrium oxide in the irradiated plates was from 3% to 15%. For getting optical smoothness, prior to illumination all samples were subjected to mechanical polishing, after which the level difference between surface cavities and asperities was at most 20 nm (Fig. 1).

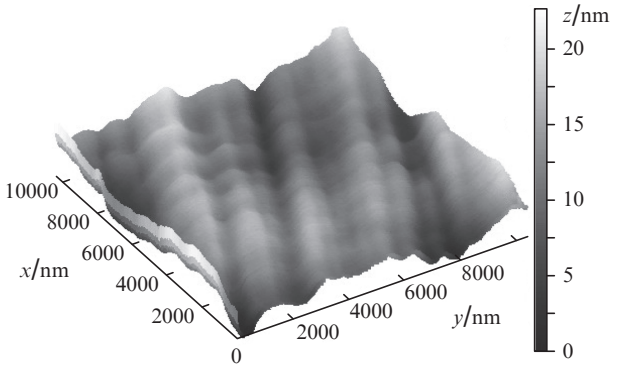

Figure 1. 3D photograph of the surface of a ZrO_2 sample subjected to mechanical polishing (prior to irradiation) obtained by AFM.

A high-intensity beam with a uniform distribution of the radiation intensity on the surface of the irradiated sample was produced by the projection system described elsewhere (see, for example, [8]) which comprised a condenser lens with a focal length of 250 mm, a molybdenum mask, and a projection lens with a focal length $f = 50$ mm (Fig. 2). The round molybdenum mask of diameter 0.5 mm was projected by the projection lens with a five-fold demagnification exactly onto the surface of the sample. If needed, only the most uniform central part was selected by diaphragm (*2*) and mask (*4*) from the direct beam.

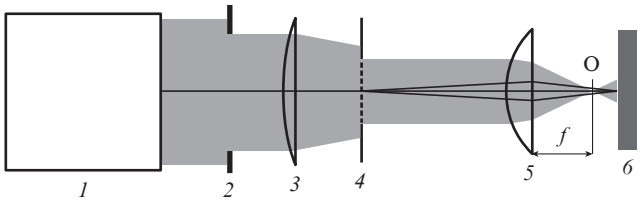

Figure 2. Scheme of the optical setup with a projection system for laser irradiation of the material: (*1*) ArF laser; (*2*) diaphragm; (*3*) condenser lens; (*4*) diaphragm projected with demagnification to the surface of the material; (*5*) projection lens; (*6*) irradiated material; O is the focus of lens (*5*). For clearness, all angles between rays and the optical axis are enlarged.

Surfaces of irradiated samples were examined by a Solver P47 atomic-force microscope (AFM) and a scanning electron microscope.

Photographs of the surface structure of zirconium dioxide after multiple (30–40 pulses) laser irradiation at a relatively low energy density of the laser pulse are presented in Figs 3 and 4. Neither surface melting nor evaporation removal of the material is observed; however, a new relief distinct from initial is produced.

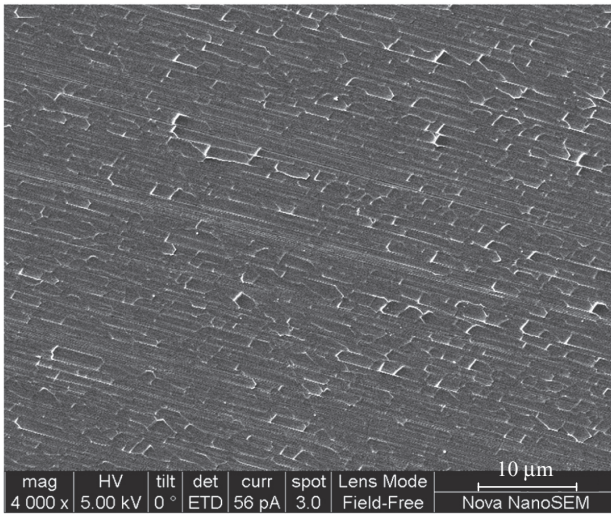

Figure 3. SEM photograph of the surface structure of zirconium dioxide after irradiation by 30 ArF-laser pulses at a relatively low energy laser pulse density (0.14 J cm^{-2}).

In Fig. 3, on the surface irradiated by 30 pulses with the energy density of 0.14 J cm^{-2} one can see only cracking of the surface layer without any noticeable lamination. Figure 4 shows a SEM-photograph of the surface irradiated at an energy density greater (0.23 J cm^{-2}) than that in Fig. 3. In contrast to Fig. 3, one can see not only cracking, but also lamination of characteristic thin bordered-up flakes. One can also see thin (~100 nm) submicron cracks between the flakes. The characteristic dimensions of flakes along the initial surface are from 1 to 5 μm.

The photograph of the surface irradiated at a greater laser energy density (0.29 J cm^{-2}) shown in Fig. 5 was obtained by AFM. In this case, flakes not only peel off but also fly away from the surface leaving on it characteristic barriers of height 300–600 nm. In addition, at the mentioned sufficiently high

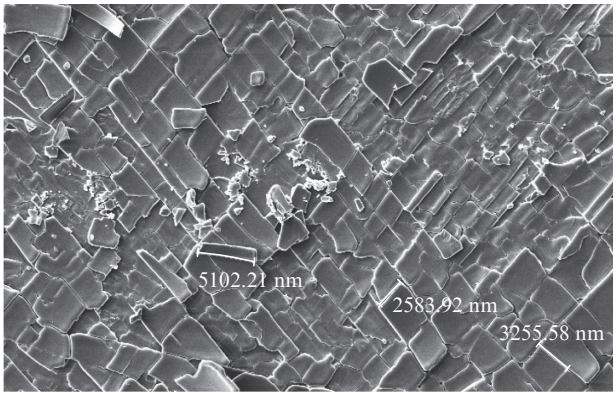

Figure 4. SEM photograph of the surface of zirconium dioxide after irradiation by the ArF laser at the pulse energy density of 0.23 J cm^{-2}.

energy density of 0.29 J cm^{-2}, relief melting becomes visible, which is manifests itself in rounding of the barriers mentioned above (Fig. 5) and acute angles of flakes (see the SEM-photograph in Fig. 6) due to capillary forces.

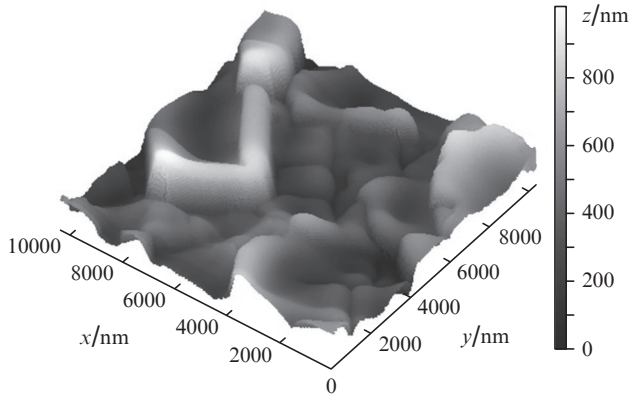

Figure 5. AFM photograph (3D) of the surface of zirconium dioxide after irradiation by the ArF laser at the pulse energy density of 0.29 J cm^{-2}.

3. Discussion of results

The shape of quasi-periodic micron and submicron structures arising under laser irradiation (Figs 3 and 4) indicates material deformation due to thermal stresses without melting at least at the laser energy density of $F < 0.29$ J cm^{-2}.

One may attempt to roughly estimate the temperature at which the near-surface layer starts to crack in the case shown in Fig. 3, where $F = 0.14$ J cm^{-2}.

To simplify the estimates, we will assume below that the laser pulse is rectangular and thermo-physical and optical parameters are independent of temperature. In this case the temperature of the material surface under the action of laser pulses can be estimated by the formula

$$T = \frac{AF}{\rho C \delta} + T_{\mathrm{i}}. \qquad (1)$$

Here A is the absorbing capability of the material surface; ρ is the density of 'fianite'; C is its specific heat; and T_{i} is the initial

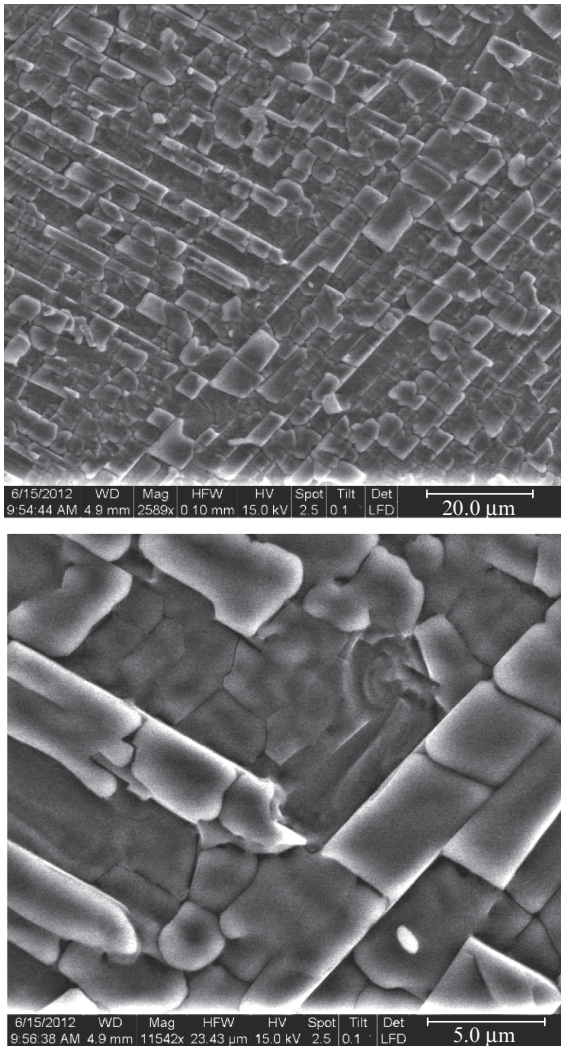

Figure 6. SEM microphotograph with various magnifications of the surface of a stabilised zirconium dioxide crystal sample (ZrO_2 + 10%Y_2O_3) after multiple (30 pulses) irradiation with the pulse energy density $F = 0.29$ J cm^{-2}. One and the same surface area was irradiated.

temperature of the surface. The parameter δ, as follows from the theory of heat conduction [9], is the thickness of the effective zone in the material where heat is released during the pulse duration τ, which is equal to a maximal of the two values $1/\alpha$ and $(\pi\chi\tau)^{1/2}/2$:

$$\delta = \max[1/\alpha; (\pi\chi\tau)^{1/2}/2], \tag{2}$$

where α is the absorption index (in cm^{-1}); $1/\alpha$ is the depth of absorption; and χ is the thermal diffusivity of the material (in cm^2 s^{-1}).

However, we cannot directly use formula (1) for estimating the temperature of the material surface because many of the parameters included in (1) are not constant. The temperature rise induced by laser heating up to the melting temperature T_m (2715 °C) or evaporation temperature T_v most noticeably (by an order of magnitude and greater) may change the absorption index α, which can both increase and decrease, and thermal diffusivity of the material χ, which usually decreases at elevated temperatures. The values of the parameters at high temperatures usually are not known, which is a general problem in analysing the interaction of intensive radiation with matter. Correspondingly, the parameter δ in (2) has a large uncertainty and cannot be calculated from reference data given for room (initial) temperature or for moderate temperatures, which for refractory ceramics are noticeably lower than the melting temperature.

In view of these facts we will roughly estimate the parameter δ by using available experimental measurements of the melting threshold of the material $F_m = 0.29$ J cm^{-2}. Indeed, the melting threshold F_m can be found from the relationship [9]

$$F_m = \frac{\rho C(T_m - T_i)\delta}{A}, \tag{3}$$

which for finding δ can be rewritten in the form

$$\delta = \frac{AF_m}{\rho C(T_m - T_i)}. \tag{4}$$

After substituting the average reference data $A = 0.8$ (for the optical constants $n = 2.6$ and $k \ll 1$), $\rho = 5.8$ g cm^{-3}, $C = 450$ J (kg K)$^{-1}$, $T_m = 2750$ °C, $T_i = 20$ °C and the experimental value for melting threshold $F_m = 0.29$ J cm^{-2} we obtain the effective average value $\delta = 330$ nm. Note that at the wavelength equal to this value, according to (2), the absorption index is $\alpha = 3\times10^4$ cm^{-1}, which is an order of magnitude close to the value of α given in [10] for room temperature (about 10^5 cm^{-1}).

By substituting $\delta = 330$ nm to expression (2) one may calculate the surface temperature T^* attained at $F = 0.14$ J cm^{-2}, i.e., at the threshold of surface cracks (at the same parameters of A, ρ, C, T_m, and T_i): $T^* = 1320$ °C.

Note that the thickness (300–600 nm) of peeled-off flakes (see Fig. 5) agrees with the obtained value $\delta = 330$ nm by an order of magnitude, and the threshold temperature for surface cracking $T^* = 1320$ °C is close to the value of the temperature known from literature [11] for the phase transition in unstable zirconium dioxide from monocline to tetragonal crystal structure $T_{ph} = 1170$ °C, at which the negative change of volume occurs by 3%–5%. Such volume change in a solid state phase under heating the sample favours conditions for cracking the near-surface layer to a depth of, at least, δ because this most heated layer, due to the negative change of volume, gets a stretched and stressed state in contrast to the underlying 'cold' mass of the material.

The characteristic orientation of cracks in certain directions along the surface may be explained by anisotropy of thermo-elastic strength parameters of a particular material (the limits of the material strength are minimal along certain directions due to anisotropy).

Characteristic micron dimensions of flakes along the material surface are explained by the temperature stress relaxation model.

Under the action of intensive laser radiation, high temperature stresses arise in solids. In these conditions, the deformation process is accompanied by a residual deformation which is related to nonelastic effects and rearrangement of the crystal defect structure. Relaxation of stresses may be of heterogeneous character due to generating in the old excited structure a new structure of relaxation zones [12]. This is related to a collective behaviour of interacting excited atoms, which makes the relaxation process nonlinear. Depending on the state of the system, conditions of external action, degree of evolution of the deformation process, the relaxation zones may arise from centres of new phase, groups of dislocations

(or disclination groups), micro-cracks, and groups of atoms or vacancies forming clusters, micro-pores, dislocation loops, etc. Generally, zones should be distributed in size. We will assume that the process of relaxation forms zones of equal dimensions.

The nonequilibrium state of an elastically deformed solid is determined by temperature T, tensor of deformation ε_{ij} or stresses σ_{ij} and a set of additional internal parameters of state $\psi_{ik}^{(1)}$, $\psi_{ik}^{(2)}$, …, $\psi_{ik}^{(N)}$, specifying the degree of system deviation from the equilibrium state at prescribed T and ε_{ik}. The number of the internal state parameters $\psi_{ik}^{(\alpha)}$ is such that, combined with T and ε_{ik}, they completely determine the system state. The parameters $\psi_{ik}^{(\alpha)}$ are second-rank tensors; we may call them ordering parameters.

To analyse the behaviour of a deformed solid body one should find the expression for a thermodynamic potential F as an explicit function of T, ε_{ik}, and $\psi_{ik}^{(\alpha)}$. For an isotropic solid [12]

$$\dot{\psi}_{ik}^{(\alpha)} = 2D^{(\alpha)}\psi_{ik}^{(\alpha)} + 4F^{(\alpha)}(\psi_{ik}^{(\alpha)})^3, \tag{5}$$

$$F = \frac{k}{2}(\varepsilon_{\text{II}}^2 + \varepsilon_{\text{II}}^4) + \sum_{\alpha} D^{(\alpha)}(\psi_{ik}^{(\alpha)})^2 + \sum_{\alpha} F^{(\alpha)}(\psi_{ik}^{(\alpha)})^4. \tag{6}$$

Equations (5) and (6) determine the behaviour of a deformed solid body in the conditions of stress relaxation. However, they are of general character because in deriving them we actually used no model representation. This implies both advantages and drawbacks not only for this but for any other phenomenological theory. To make clear a physical sense of the parameters included in (5) and (6) and determine their values it is reasonable to consider a particular model example. First of all, we present the entire set of relaxation parameters $\psi_{ik}^{(\alpha)}$ as a single parameter. As such we will take the residual deformation $\varepsilon_{ij}^0(r,t)$ and introduce the mesoscopic relaxation parameter determining the relaxation process field,

$$\phi_{ik}(r,t) = \frac{1}{V_0}\int_{V_0} \varepsilon_{ik}^0(r,t)\,\mathrm{d}V,$$

where V_0 is the volume over which $\varepsilon_{ik}^0(r,t)$ is averaged. Thus, the considered scheme – deformed solid body – may be presented in the form of three simultaneously co-existing phases: the relaxation field determined by the parameter $\phi_{ij}(r,t)$, the field of stresses $\sigma_{ij}(r,t)$ corresponding to external loads, and relaxation zones with a concentration n.

Time evolution of $\phi_{ik}(r,t)$, $n(r,t)$, and $\sigma_{ij}(r,t)$ is determined by the system of nonlinear differential equations

$$\begin{aligned}
\dot{\phi}_{ik} &= -\kappa\phi_{ik} + g_1 n \\
\dot{n} &= -\gamma n + \frac{\phi_{ik}\sigma_{ik}}{g_2} \\
\dot{\sigma}_{ik} &= \nu(\sigma_{ik} - \sigma_0) - g_3\phi_{ik}n.
\end{aligned} \tag{7}$$

The first summands in the right sides of these equations describe, correspondingly, attenuation of relaxation process, decay of generated relaxation zones, and relaxation of stresses in a linear approximation without mutual interaction. The second summands make the process of relaxation nonlinear. In the first equation the summand is related to generation of the relaxation field due to formation of relaxation zones. In the second equation, an influence of the relaxation field $\phi_{ik}(r,t)$ and the stress field $\sigma_{ij}(r,t)$ on generation of relaxation zones is taken into account. In the third equation the second summand is related to an influence of the relaxation field and of relaxation zones on the relaxation of stress rate. Here, ν, γ, κ, g_1, g_2, g_3 are material constants. The value of σ_0 is determined by applied external loads and corresponds to the steady residual stress established in the result of relaxation.

The rate of variation in the relaxation field is substantially lower than the rate of atom relaxation processes described by the constants γ and ν. Hence, in (7) we may use adiabatic elimination of variables. As a result we obtain the relaxation equation with defined constants:

$$\dot{\phi}_{ik} = A\phi_{ik} - B\phi_{ik}^3,$$

where

$$A = \frac{g_1}{g_2\gamma}\left(\sigma_0 - \frac{g_2\gamma}{g_1}\kappa\right);\ B = \frac{g_1 g_3}{g_2^2}\frac{\sigma_0}{\gamma^2\nu}.$$

This approach makes no allowance for the possible fluctuations of the relaxation parameter, whose role increases at higher loads and temperature. With these fluctuations taken into account the kinetic equation for the relaxation parameter is written in the form

$$\dot{\phi}_{ik} = A\phi_{ik} - B\phi_{ik}^3 + D\Delta\phi_{ik}. \tag{8}$$

Here, D is the diffusion coefficient for atoms in a heated zone. If we take into account the dispersion of diffusion, then Eqn (8) reduces to the generalised Ginzburg–Landau equation [13]. At

$$\sigma_0 < \frac{g_2\gamma}{g_1}\kappa,$$

Eqn (8) has a single stable solution $\phi(r,t) = 0$. If the critical value is violated

$$\sigma_0 \geqslant \sigma_{\text{cr}} = \frac{g_2\gamma}{g_1}\kappa,$$

then new 'coherent' states of the system are realised, which are closer to periodical, that is are quasi-periodical. The period of such a structure is

$$T = \frac{\sigma_0 - \sigma_{\text{cr}}}{2\pi\sigma_0}\sqrt{\frac{3}{8}\frac{D}{\nu}}. \tag{9}$$

In order to estimate numerically T by formula (9) in the case of pulsed laser radiation acting on the surface of zirconium dioxide, we will assume that the residual stresses are $\sigma_0 = 10^9$ N m^{-2}; $\kappa \approx \gamma \approx \nu \approx g_1 \approx 10^{-3}$ s^{-1} as determining the frequency of jumping of atoms from one equilibrium state to another (in the state of thermal equilibrium at arbitrary temperature a crystal comprises a certain number of vacancies reaching 10^{-4}–10^{-3} near the melting point [14]); $g_2 \approx g_3 \approx 10^{10}$ N m^{-2} is the stress in relaxation zones; and $D \approx 10^{-8}$ cm^2 s^{-1} is the coefficient of atom diffusion in the heated zone of the crystal (because it is known that the upper limit of measured diffusion coefficients for temperatures below the melting temperature is 10^{-8}–10^{-6} cm^2 s^{-1} [14]). After substituting into (9) we have $T \approx 3$ μm, which agrees with the results of our experiment (Figs 3–6).

Note that we considered only the case of a bulk crystal. It was assumed that generation of periodic structures in a thin near-surface layer results in the formation of corresponding structures on the surface. Note also that extension of the surface area due to formation of the micron and submicron (in thickness) structures on it may result in a greater ion flow through electrolytic membranes from zirconium dioxide and, as a consequence, to a higher efficiency of solid oxide fuel cells. Study and optimisation of this effect is a next stage of our activity.

4. Conclusions

In the present work we have experimentally demonstrated the possibility of obtaining quasi-periodic micron and submicron structures on the zirconium dioxide surface irradiated by nanosecond laser pulses without surface melting.

The temperature at which a near-surface layer starts cracking is approximately estimated. It is almost twice lower than the melting temperature, and in heating it is close to the known phase transition temperature in solid zirconium dioxide from monocline to tetragonal crystal structure equal to 1170 °C. Experimentally observed characteristic orientation of cracks in certain directions along the surface may be explained by the anisotropy of thermo-elastic strength parameters of this crystal material, due to which the strength limits along certain directions of the material are minimal.

It was also shown that the submicron thickness of flakes peeling off under laser irradiation corresponds to the thickness of the effective zone of heat release in the material during the laser pulse action.

For explaining micron dimensions of the structure along the material surface, a theoretical model was suggested based on consideration of relaxation zones of temperature stresses and on solving the generalised Ginzburg–Landau equation. An estimate of the period of surface structures (about 3 μm) for zirconium dioxide by this model yields the result coinciding with experimental data (2–5 μm).

Acknowledgements. The authors are grateful to E.E. Lomonova for presented samples of zirconium dioxide, V.D. Frolov and G.V. Molodtsova for their help in AFM and SEM investigation.

The work was supported by the Federal Target Programme 'Scientists and Science Educators of Innovative Russia' in 2009-2013 (State Contract No. 16.740.11.0537).

References

1. Pereira A., Cros A., Delaporte P., Georgiou S., Manousaki A., Marine W., Sentis M. *Appl. Phys. A*, **79**, 1433 (2004).
2. Lazare S., Tokarev V.N., Sionkowska A., Kaczmarek H., Wiśniewski M., Skopińska J. *Appl. Phys. A*, **81**, 465 (2005).
3. Khomich V.Yu., Mikolutskiy S.I., Shmakov V.A., Yamshchikov V.A. *Nanotechnology in Russia*, **6** (11–12), 733 (2011).
4. Tokarev V.N., Khomich V.Yu., Shmakov V.A., Yamshchikov V.A. *Dokl. Ross. Akad. Nauk*, **419**, 1 (2008).
5. Khomich V.Yu., Urlichich Yu.M., Shmakov V.A., Tokarev V.N., Galstyan A.M., Mikolutskii S.I., Yamshchikov V.A. *Fiz. Khim. Obrabot. Mater*., **6**, 15 (2012).
6. Malkin V.S. *Fotonika*, **2**, 16 (2009).
7. Reif J., Costache F., Varlamova O., Jia G., Ratzke M. *Phys. Stat. Sol. C*, **3** (3), 681 (2009).
8. Tokarev V.N., Lopez J., Lazare S., Weisbuch F. *Appl. Phys. A*, **76**, 385 (2002).
9. Tokarev V.N., Kaplan A.F.H. *J. Appl. Phys.*, **86**, 2836 (1999).
10. Heiroth S., Ghisleni R., Lippert T., et al. *Acta Materialia*, **59**, 2330 (2011).
11. http://accuratus.com/
12. Khomich V.Yu., Shmakov V.A. *Dokl. Ross. Akad. Nauk*, **446** (3), 1 (2012).
13. Gaponov-Grekhov A.V., Lomov A.S., Osipov G.V., Rabinovich I.I., in *Nelineinye volny. Dinamika i evolutsiya* (Nonlinear Waves. Dynamics and Evolution) (Moscow: Nauka, 1989) p. 61.
14. Kalin B.A. *Fizicheskoe materialovedenie. Fizika tverdogo tela* (Physical Material Science. Solid-Body Physics) (Moscow: MEPhI, 2007).